

CR-39 TRACK DETECTORS IN COLD FUSION EXPERIMENTS: REVIEW AND PERSPECTIVES

A. S. Roussetski

P. N. Lebedev Physical Institute, Russian Academy of Sciences
e-mail rusets@x4u.lebedev.ru

Introduction

Earlier experiments [1,2] have showed emissions of DD-reaction products (3-MeV protons) and energetic charged particle emission (α -particles) during exothermic D(H) desorption from the Pd/PdO:D(H) heterostructures. The occurrence of these emissions was confirmed by independent experiments using both Si-surface barrier and CR-39 plastic track detectors [3, 4].

Over the last few years, the CR-39 track detector has become a popular method to measure charged particle emissions in cold fusion experiments. The use of CR-39 is quite simple and cheap, but this technique demands some special conditions. As shown below, the observance of these conditions allows the researcher to not only detect charged particles, but also to identify their types and estimate their energy spectrum. On the other hand, when these conditions are not met, the method can fail, mainly because of problems with radioactive nuclides contained in the surrounding materials (electrolyte, air, cathode etc.), mechanical defects, and the development process after etching.

The necessary conditions for correct CR-39 measurement include the following:

- Purification of CR-39 detector surface;
- Low density of background tracks before measurements, and protection of CR-39 from external radioactive contamination;
- Correct calibration procedure;
- Control of background during the measurement and the use of “clean” materials (without radioactive nuclides);
- Protection of detector surface from mechanical and thermal influences, high intensity UV radiation;
- In some tests, shielding foils with known stopping ranges identify particle types;
- Correct etching conditions in each measurement

Access to purified track detectors along with knowledge of track characteristics produced by various types of particle allow the use of CR-39 chips in long-duration experimental exposure during and after electrolysis with Pd and Ti cathodes. We used purified CR-39 detectors produced by Landauer Inc. (USA) and Fucuvi Chemical Industry Co (Japan) with very low background track density ($N_b < 20 \text{ cm}^{-2}$) to detect the emissions with very low intensity ($10^{-4} - 10^{-3} \text{ cm}^{-2}\text{s}^{-1}$).

CR-39 track detector

CR-39 is a polymer ($\text{C}_{12}\text{H}_{18}\text{O}_7$) with a density of $\sim 1.3 \text{ g/cm}^3$. When a charged particle crosses the detector surface it causes radiation damage along trajectory. This zone of structure damage may be increased to $10^{-4} - 10^{-2} \text{ cm}$ by etching in a chemical reagent. We used optimal etching conditions for CR-39 detector: 6N solution NaOH at 70°C over 7 h.

$V = V_T/V_B = f(dE/dx)$ – etch rate ratio (where dE/dx – stopping power of particle, V_T and V_B – track and bulk etch rates). A track is formed if $V_T > V_B$.

If $V_B = V_T$, $dE/dx = (dE/dx)_s$ – the threshold stopping power.

The critical angle of detection θ_c is determined as the minimal angle between the particle trajectory and detector surface when track formation is still possible: $\theta_c = \arcsin(V_B/V_T)$

It is easy to show that if detector crossed by particles in different directions the detection efficiency is determined as

$$\eta = 0.5 \cdot (1 - \sin \theta_c)$$

Experimental technique

The measurements were carried out using PAVICOM [4] – a completely automated device for track detector processing. It consists of an optical microscope with a digital video camera; a sample holder stand with three-dimensional displacement provided by stepper motors with accuracy of 0.25 micron; manual controls; and a personal computer for automatic measurements.

We used alpha-sources and a cyclotron alpha beam ($E_\alpha = 2 - 30$ MeV) to calibrate the CR-39. Fig. 1 shows the photomicrograph of tracks from α -particle cyclotron beam ($E_\alpha = 11$ MeV) normally incident on CR-39 detector. For proton calibration we used a Van de Graaf accelerator ($E_p = 0.6-3.0$ MeV). The results of the calibration – the dependence of track diameter from particle energy – are presented in Fig. 2 for α -particles, and Fig. 3 for protons.

We used the following types of samples in our experiments. Electrochemically loaded Au/Pd/PdO:D_x heterostructures were used for charged particle emission during deuterium desorption after electrolysis. Ti (30 μm), Pd (30 μm) cold worked foils and Pd/PdO heterostructures (50 and 100 μm) were used for in-situ measurements during electrolysis in a solution of 1M Li₂SO₄/H₂O (current density $j = 10$ mA/cm²). Pd (30 μm) and Pd/PdO (50 μm) samples with He implanted on the surface 2×10^{17} and 2×10^{16} atom/cm², respectively, were used to investigate the influence of He impurities on alpha-particle emission during electrolysis.

The example of long duration background measurements with a 0.1 M Li₂SO₄ solution is presented in Fig. 4. The main part of background tracks spaced in the range of diameters 8 – 12 μm . We can estimate the mean level of background α -emission as $\langle n_b \rangle = 2.7 \cdot 10^{-4} \text{ s}^{-1} \text{ cm}^{-2}$.

Results and discussion

The measurements with Pd/PdO (50 μm) sample after electrolysis showed that high energy charged particle emission take place not only on the whole sample surface, but also it can concentrate in some small zones (“hot zones”) with dimensions of a few hundred microns corresponding to places with maximum internal strains. The photomicrographs of “hot zone” (250 \times 500 μm^2) with $\sim 10^3$ tracks of α -particles and protons are showed in Fig. 5a,b. The distribution of track diameters for particles normally incident to the detector is showed in Fig. 6. We can see three peaks that corresponded to following particles and energies: $d = 6.0 - 6.5 \mu\text{m}$ ($E_p = 1.4 - 1.7$ MeV), $d = 7.0 - 7.6 \mu\text{m}$ ($E_\alpha = 9.2 - 14.0$ MeV), $d = 7.8 - 8.6 \mu\text{m}$ ($E_p = 5.6 - 7.8$ MeV).

The distribution of track diameters for the entire detector surface (not just in the “hot zone”) is presented in Fig. 7. We observe the same peaks in this distribution. This means that the charged particle emission in the “hot zone” is the same as the rest of the sample, but the emissions are concentrated in space (and, possible, in time). We estimated the mean intensity of charged particle emission (protons and α -particles, without “hot zone”) during all time of exposition (5 h) as $\langle n \rangle = 6 \times 10^{-2} \text{ s}^{-1} \text{ cm}^{-2}$.

We also observed some rare events when 3 or more α -particles emitted from one point on the sample surface. We observed such events both after electrolysis and during long duration electrolysis measurements. Examples of these events with Au/Pd/PdO:D_x (40 μm) and PdHe (30 μm , 2×10^{17} atom He/cm²) samples are presented in Figs. 8 and 9, respectively. In these cases we can estimate the energy of emitted α -particles, measuring their ranges from the point of emission to the end of tracks. Taking into account the thickness of detector shielding (50 and 60 μm PE, respectively) and etched layer of CR-39 ($\sim 9 \mu\text{m}$), we can estimate the energies of

emitted α -particles: $E_{\alpha 1} = E_{\alpha 2} = 11.2$ MeV; $E_{\alpha 3} = E_{\alpha 4} = 9$ MeV; $E_{\alpha 5} = E_{\alpha 6} = 8.3$ MeV; $E_{\alpha 7} = 10$ MeV (see Fig. 8) and $E_{\alpha 1} = 9.2$ MeV; $E_{\alpha 2} = 8.6$ MeV; $E_{\alpha 3} = 9$ MeV; $E_{\alpha 4} = E_{\alpha 5} = E_{\alpha 6} = 8.4$ MeV (see Fig. 9). The energies of all these α -particles are more than energies of natural background and they can be identified as long range particles emitted from the sample surface under high internal strains. These events demonstrate the release of few tens MeV of energy concentrated in small volume of sample. If we suppose that the energy concentrated in the region compared with dimension of the lattice, and released in a time period of $10^{-12} - 10^{-14}$ s, we get the power $\sim 10^{18} - 10^{20}$ W/cm².

Conclusion

1. We formulated the necessary conditions for successful using of CR-39 detector in typical cold fusion experiments, include electrolysis, H/D desorption and glow discharge.
2. It was shown that CR-39 can be used to measure the intensity of emitted charged particles, to determine their type, and to estimate their energies.
3. We found active zones (“hot zones”) on the sample surface visible as areas with high density of charged particle tracks.
4. We observed the emission of three or more alpha particles from one point on the sample surface, suggesting the correlation of space and possibly time between these events. These events assume the emission of high energy (20 - 50 MeV) on small areas of the sample surface comparable with the dimensions of lattice. These indicate the power density $\sim 10^{18} - 10^{20}$ W/cm², which is comparable to the power density of intensive picosecond laser emission.

References:

1. A. G. Lipson et al. Fusion Technology **38**, 238 (2000)
2. A. G. Lipson, B.F. Lyakhov, A.S. Roussetski. Proc. ICCF-8, Italian Phys. Soc. Conference Proc. **70** (2001) 231
3. A. G. Lipson, A.S. Roussetski et al. Bulletin of the Lebedev Physics Institute Russian Academy of Sciences. 2001, v10, 22.
4. A. G. Lipson, A.S. Roussetski, C.H. Castano and J. Miley. Bull. of Amer. Phys. Soc. v47, (2002) 1219.
5. A. B. Aleksandrov et al, Nucl. Instr. And Meth. A535 (2004) 542-545.

Figures

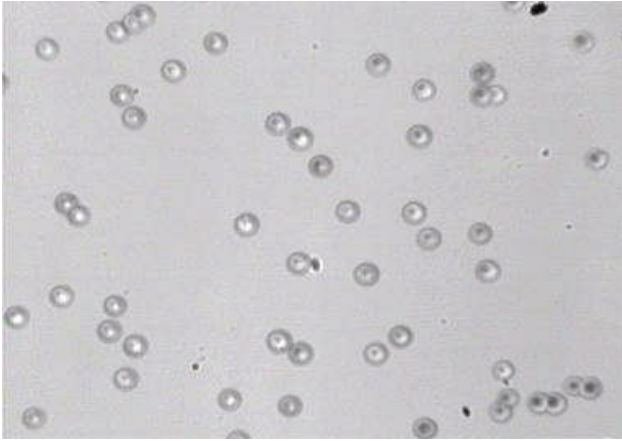


Fig. 1. Tracks from α -particle cyclotron beam ($E\alpha = 11$ MeV) normally incident on CR-39 detector. Image size – $120 \times 90 \mu\text{m}$

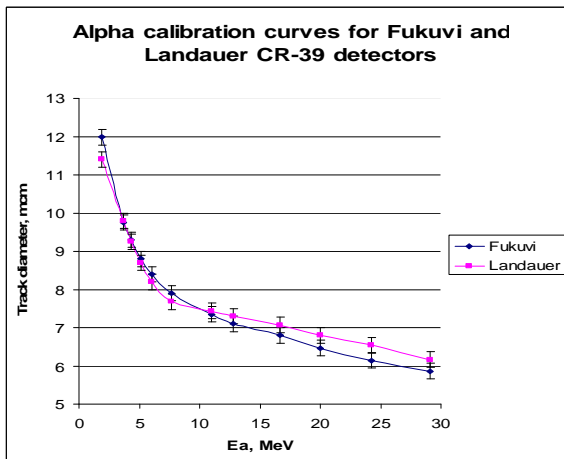


Fig. 2. Alpha-sources and cyclotron alpha beam calibration (2-30 MeV) of CR-39.

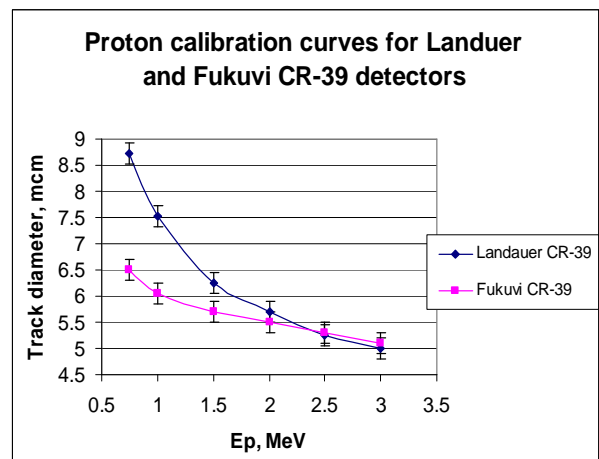


Fig. 3. Proton calibration with Van-DeGraaf accelerator (0.6-3.0 MeV).

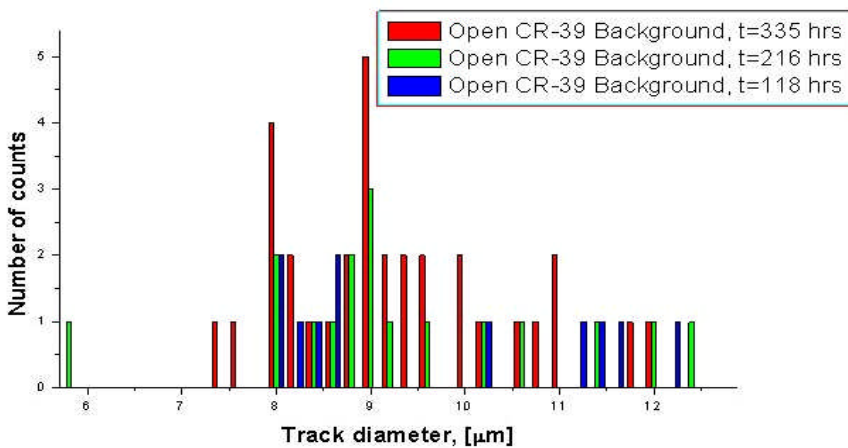


Fig. 4. Example of background during electrolysis in $0.1 \text{ M Li}_2\text{SO}_4$.

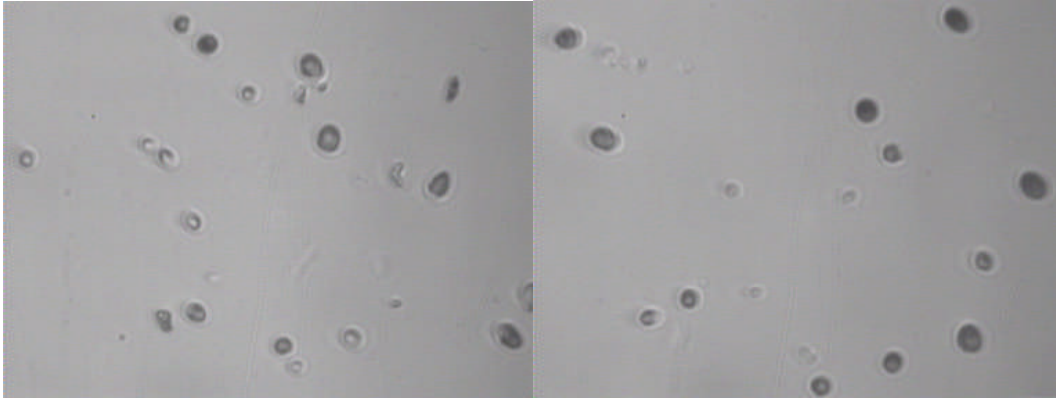


Fig. 5a,b. CR-39 measurement after electrolysis of Pd/PdO:H_x (50 μm). Shielding of CR-39 – 11 μm of Al. Photomicrographs of “hot zone” (250 × 500 μm²) with tracks of α-particles and protons. Image size – 120 × 90 μm

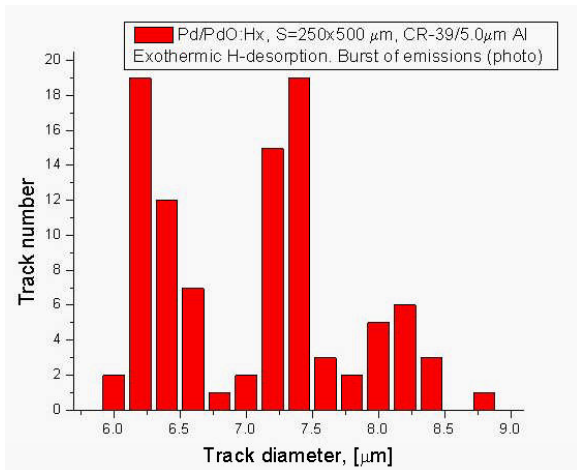


Fig. 6. Distribution of track diameters in “hot zone” (250 × 500 μm²)

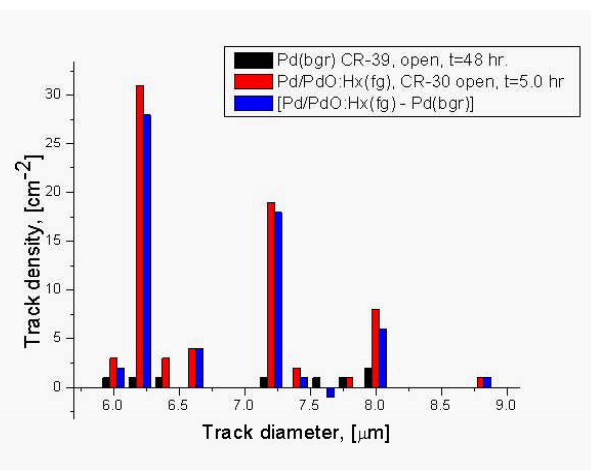


Fig. 7. Distribution of track diameters on CR-39 surface without “hot zone”

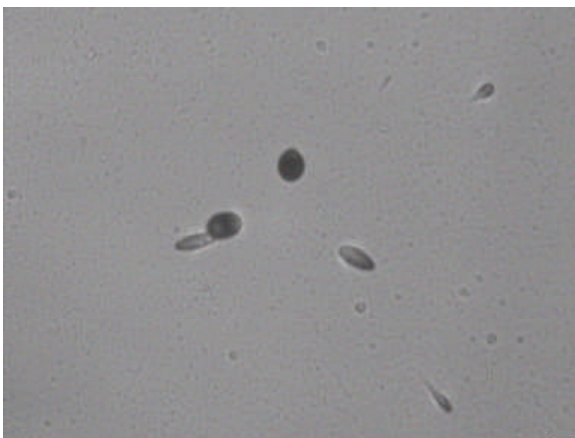


Fig. 8. CR-39 measurements after electrolysis of Au/Pd/PdO:Dx. Shielding of CR-39 – 50 μm of PE. Image size – 240 × 180 μm. 7 α-particle emission from one point on the sample surface.

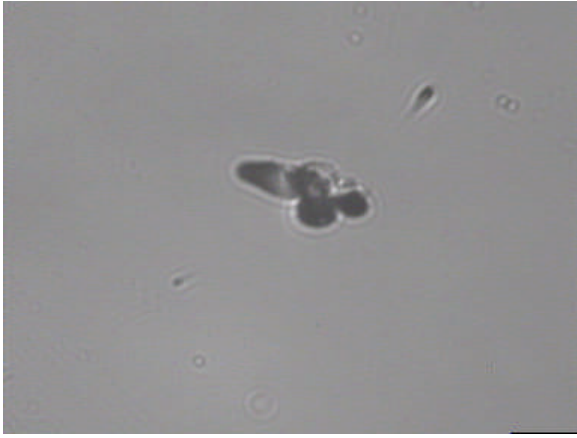


Fig. 9. CR-39 measurements during electrolysis of PdHe ($30\ \mu\text{m}$ thick, $2 \times 10^{17}\ \text{He}/\text{cm}^2$) in $1\text{M}\ \text{Li}_2\text{SO}_4$ ($j = 4\text{-}40\ \text{mA}/\text{cm}^2$). Shielding of CR-39 – $60\ \mu\text{m}$ of PE. Image size – $120 \times 90\ \mu\text{m}$
6 α -particle emission from one point on the sample surface